Citation Ahmad Mustafa, Klaas Koster, and Ghassan AlRegib, 2023, "Explainable Machine Learning for Hydrocarbon Prospect Risking." accepted for publication to Geophysics.

DOI Will be updated once it is available

Review Received acceptance notification on 19th June, 2023.

Data Data and Codes are proprietary and not available.

Bib Will be updated once it is available

Contact Ahmad Mustafa, Klaas Koster, and Ghassan AlRegib (amustafa9@gatech.edu, klaas_koster@oxy.com, and alregib@gatech.edu)

Explainable Machine Learning for Hydrocarbon Prospect Risking

Ahmad Mustafa*, Klaas Koster†, and Ghassan AlRegib*

ABSTRACT

Hydrocarbon prospect risking integrates information from multiple geophysical data and modalities to arrive at a probability of success for a given prospect. The DHI database of drilled prospects gathers data from prospects drilled around the world in multiple geologic settings in one central knowledge base. A major goal of interest to geophysicists is to understand the impact of various seismic amplitude anomalies, that are interpreted as direct hydrocarbon indicators, on the risking process. The individual correlation-based analysis typically carried out for this purpose misses out on complex feature interactions governing the physical phenomena. Data-driven machine learning techniques have the potential to sift through large, multi-dimensional datasets to learn mappings from feature spaces to outcome classes. LIME is a model explainability technique that explains decisions by black-box models by locally approximating their behavior. We propose a novel method whereby LIME is used in conjunction with various machine learning models to learn mappings from feature spaces in the DHI database to respective prospect outcomes. Consequently, we are able to highlight seismic amplitude anomalies considered most important by the models to the risking process and we show that our insights agree with geophysical intuition. Moreover, we use LIME explanations to demonstrate a case study of bias detection with machine learning models for the application of prospect risking. A limitation with LIME is that it only explains model behavior around solitary datapoints. Towards this end, we propose novel metrics summarizing a model's global understanding of a dataset by aggregating local explanations over individual examples. To the best of our knowledge, this is the first work using explainable machine learning for the purpose of bringing novel insights to prospect risk assessment.

*Center for Energy and Geo Processing (CeGP), Omni Lab for Intelligent Visual Engineering and Science (OLIVES), School of Electrical and Computer Engineering, Georgia Institute of Technology, Atlanta, GA. † Occidental Petroleum, Greenway Plaza, Houston, TX.

INTRODUCTION

Machine learning and other data-driven methods feature prominently in several geophysics applications and have begun to become a central component in routine tasks. For example, data-driven machine learning methods have been used for solving problems in salt body delineation (Wang et al., 2015; Amin et al., 2017; Shafiq et al., 2017; Di et al., 2018b), fault detection (Di and AlRegib, 2019; Di et al., 2019a,b), facies classification (Alaudah et al., 2019b,c), seismic attribute analysis (Long et al., 2018; Di et al., 2018a; Alfarraj et al., 2018), and structural similarity based seismic image retrieval and segmentation (Alaudah et al., 2019a). Advanced machine and deep learning concepts have also specifically been used to deliver performance in labeled data-constrained environments such as seismic inversion (Alfarraj and AlRegib, 2019; Biswas et al., 2019; Mustafa et al., 2019; Mustafa and AlRegib, 2020, 2021).

However, a major hurdle in the wider adoption of advanced machine learning-based methods for geophysics and a variety of other real world applications has been the dilemma of their inherent black-box natures. While data-driven methods have been known to outperform simpler models and human beings at certain tasks (McKinney et al., 2020), the reasoning employed by them to arrive at their decision is seldom transparent to end users. The ramifications of the matter were serious enough for the European Commission to stipulate the need for algorithmic processes to provide explanations about their decision to the persons involved (Bibal et al., 2020). In applications involving considerable ethical and legal considerations (e.g., bank loan application processing, hiring, crime monitoring and prediction, medicine etc.) the need for machine learning algorithms to be interpretable and explainable can not be overstated for two main reasons: firstly, it would lead to increased user trust in the decision systems and secondly, it would help mitigate the effect of discrimination against marginalized communities stemming from machine learning models trained on biased datasets (Fuchs, 2018). In addition, having models provide their reasoning process on tasks involving large, multidimensional datasets has the potential to uncover novel scientific insights to be further tested on in lab settings (Roscher et al., 2020).

While there is no one exact definition for explainability and interpretability in the context of machine learning currently being used in the community (Tjoa and Guan, 2021), several researchers have attempted to summarize the literature in this nascent field to articulate broad definitions and categorizations. In the work by AlRegib and Prabhushankar (2022), the authors address explainability for neural networks by framing it as the response to abductive reasoning-based questions. Specifically, post-hoc model explainability is defined as the set of methods used to obtain explanations from a trained model after it has already made a certain decision on a given data point. By systematically querying the model in an abductive fashion, explanations are generated for the model decision to highlight correlations in the data point leading to the observed decision, the feature changes needed to reverse the decision, and finally, changes needed to obtain a desired decision different to the one obtained. These explanations are obtained as the responses to the questions of *Why P?*, *Why not P?*, and *Why P rather than Q?*, respectively.

Another way to categorize explainability approaches is in terms of if they explain the complete model workings (global explanations) versus those that only attempt to explain a model in small local neighborhoods (local explanations) (Du et al., 2019). Local explanations are helpful in that they need not require any knowledge of the inner model workings and could explain a model's decision simply by locally approximating its behavior. Grad-CAM, a popular explainability technique for deep neural networks, explains model decisions on images by bringing out the pixel features most correlated with the predicted class (Selvaraju et al., 2017). Another work that builds on top of Grad-CAM uses the *'Why P rather than Q?'* framework outlined above to generate visual explanations for individual network decisions (Prabhushankar et al., 2020). For tabular datasets, locally interpretable model-agnostic explanations (LIME) has proved to be a popular option in terms of providing a tool to analyze individual model decisions using the *'Why P?'* framework (Zhang et al., 2019).

Hydrocarbon prospect risking is an application involving an immense amount of financial risk to any exploration venture. For each potential prospect in a company's drilling portfolio, information from a variety of sources and modalities is integrated to arrive at a value for the probability of finding flowable hydrocarbons. This includes an appraisal of petroleum system elements in the area(e.g., source, reservoir, trap etc.) followed by a calibration of the initial estimate by incorporating information from various seismic amplitude characteristics weighted by data quality factors. The result is a comprehensive evaluation system that thoroughly incorporates information from all modalities in an objective manner to arrive at a probability of success for the prospect of interest. The process is outlined in Figure 1 and described in Roden et al. (2012). A major goal of interest to geophysicists is to understand how various seismic amplitude anomalies impact the risking process. By statistically correlating individual attributes to post-drill results in a database of drilled prospects, Roden et al. (2012) generated attribute importance rankings for both class 3 and class 2 wells. Amplitude downdip conformance (see Figure 2) and amplitude consistency in the mapped target area were identified to be important attributes across both classes. Similarly, Roden et al. (2014) identified the most important AVO characteristics for prospect risk assessment.

A limitation with current methods is that they correlate attributes to drill outcome independently of other attributes. While this may work for datasets with small

feature sizes, it quickly becomes infeasible for large multidimensional datasets. Specifically, there may be complex feature interactions that get missed out in a simple correlation-based analysis. We propose *a novel method to learn underlying feature relationships governing both successful and failure drill outcomes for prospect risking.* This is achieved using the feature extraction capabilities of data-driven, machine learning methods combined with model decision explanations. Using the proposed novel methodology, we are able to:

1. reveal underlying feature correlations for individual cases in a prospect database,
2. use the said explanations for selecting the most important features for risk assessment in a way that agrees with prior geophysical knowledge,
3. demonstrate a case study whereby we are able to detect bias in a machine learning model trained on a prospect dataset with spurious correlations, and
4. propose and demonstrate novel metrics to summarize a machine learning model's global understanding of a dataset by aggregating local explanations for individual datapoints.

HYDROCARBON RISK ASSESSMENT

Prospect evaluation to determine the risks associated with finding hydrocarbons by incorporating all pertinent data forms an important component of exploration companies' work processes. A proper evaluation of a company's drilling portfolio allows it to rank prospects in terms of their chances of success, thereby minimizing failure rates and enhancing value for the company. Central to this risk assessment process is a quantity termed probability of geological success (Pg). Pg, expressed in percentage, represents the chance of finding hydrocarbons in a reservoir capable of sustained flow (Rose, 1992). The calculation of Pg involves a comprehensive examination of the various play elements constituting a petroleum system and then assigning a probability to each (Nosjean et al., 2021). While the exact number of such elements might vary from one company to another, they all essentially entail looking for source and reservoir rocks, the presence of a migration pathway, and closure and containment factors. The final risk is computed by independently multiplying the probabilities associated with each play element.

However, as noted by Nosjean et al. (2021), even with this evaluation system in place, there are considerable irregularities and subjective biases affecting the final Pg estimate. Specifically, the presence of seismic amplitude anomalies interpreted as direct hydrocarbon indicators (DHIs) can significantly bias interpreters to predict higher chances of success for high risk prospects and not predict high enough chances of success for prospects with numerous positive DHI characteristics. The DHI Consortium set up in 2001 collected a prospect database contributed to by over 85 companies (H.Pettingill, personal communication, 2022) with the aim to systematically understand the significance of various seismic amplitude anomalies as DHIs (Roden et al., 2012). A comprehensive knowledge base was developed where information related to geologic settings, seismic and rock physics data quality, DHI characteristics, and calibration of drilling results was all incorporated into one central library of drilled prospects.

In light of the consortium's findings, a systematic method was put in place to calculate prospect risk by minimizing much of the subjectivity associated with past works. The workflow can be summarized as shown in Figure 1. One of the first steps in the process is the computation of a quantity called initial Pg based off geological and other related information to determine the probabilities associated with each of the play elements described earlier. This is done independently from a study of the seismic amplitude anomalies to prevent a biasing of the estimated Pg. A second quantity used to inform the final Pg is the DHI index: a number computed by appraising the various seismic amplitude anomalies (e.g., flat spots, bright spots etc.) interpreted as DHIs. While the presence of DHIs can prove to be a decisive factor in terms of the final evaluation of the prospect, it is commonly known that seismic amplitude anomalies may be caused by other than the presence of hydrocarbons. It is therefore also important to adequately rate and integrate the qualities of the various geophysical data into the risking process (Forrest et al., 2010).

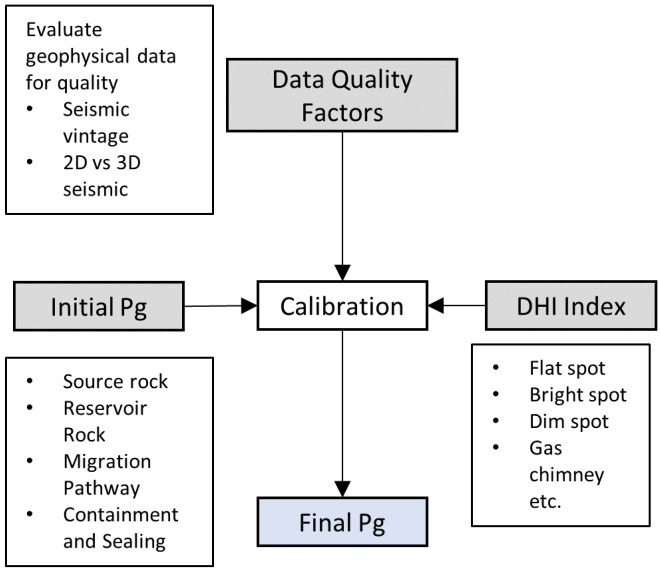

Figure 1: Risk assessment process as laid out in the work by Roden et al. (2012).

The database, presently consisting of over 360 prospects, contains wells from a variety of AVO classes (Roden et al., 2014) and geographical locations. Classes 3, 2 constitute

the bulk of prospects, with a few from class 1 and 4 settings. Around 40% of the prospects are located in the Gulf of Mexico. In addition to obtaining values for initial Pg, DHI index, data quality factors, and final Pg for each prospect, the DHI database also contains interpreter gradings of each prospect on a variety of seismic amplitude anomalies. For each characteristic, the interpreter is made to assign a grade to the prospect on a scale from 0 to 5. The higher the grade, the more the chances of the amplitude characteristic being a DHI and vice versa. An example of one such attribute (amplitude downdip conformance) along with the grading criteria established for it is shown in Figure 2.

LOCAL INTERPRETABLE MODEL-AGNOSTIC EXPLANATIONS

The local interpretable model-agnostic explanations (LIME) framework attempts to explain a black-box model f by fitting an interpretable model $g \in G$ in the locality of individual predictions made by the black-box model. G refers to the set of interpretable models g is a part of. Since it is unlikely the global behavior of a complicated model f could be captured by a simpler, interpretable model g, LIME thus seeks to only explain predictions by f on individual data points, where the explanations could be different from one sample to the next. This idea of the interpretable model being locally faithful to the original black-box model is captured in the term $\mathcal{L}(f, g, \pi_x)$. Here, x represents the data point one is interested to explain and π_x the local neighborhood around x. f and g are the original black-box and fitted interpretable models, respectively. In addition to the fidelity term $\mathcal{L}$, there is an additional penalty $\Omega(g)$ placed upon g to represent the degree of interpretability as desired for the generated model explanation. The LIME explanation for a given data point x may then be mathematically formulated as the optimization problem

$$\mathcal{E}_x = \arg\min_{g \in G} \mathcal{L}(f, g, \pi_x) + \Omega(g), \tag{1}$$

where $\mathcal{E}_x$ represents the explanation for data point x obtained by searching over the space of interpretable models G for the solution g that maximizes both the fidelity of explanation to the original model f (captured in the term $\mathcal{L}$) and the interpretability of the explanation obtained (captured in the term Ω). Below, we shed light over the details for each of the terms in the optimization problem stated in equation 1.

Feature Space Sampling for Capturing Model Decision Boundary

In order to capture the behavior of f's decision boundary in the locality of the given data point x, LIME randomly perturbs the feature space of x to generate a set of new data points $\mathcal{Z} = \{z'\}$. Using f as a black-box model, it then obtains its predictions over this dataset. The interpretable model g is then trained to learn a mapping from the feature space $\mathcal{Z}$ to the labels as generated by f. While the exact form for $\mathcal{L}$ could take different forms depending on the application, a popular choice that is also used by us in this work is the square error formulation given as

$$\mathcal{L}(f, g, \pi_x) = \sum_{z' \in \mathcal{Z}} \pi_x(z')(f(z') - g(z'))^2, \tag{2}$$

where $\pi_x(z)$ is a weighting function that weighs each sampled point z' according to its distance D from the original data point x. Since points lying closer to x are more important in terms of determining f's decision boundary in the neighborhood, they are accordingly assigned more weight in the loss terms compared to points lying further away from x. A simple choice for the weighting function could be the exponential kernel function

$$D(x, z') = \exp(\frac{-(x - z')^2}{\sigma^2}), \tag{3}$$

where σ is a preset hyperparameter controlling the sensitivity of a sample point's distance from the original to the loss function $\mathcal{L}$.

Regularization for Interpretability

The strength of interpretability in the space of searchable models G could vary. Hence, the penalty $\Omega(g)$ is placed as a constraint during optimization to bias the solution towards more interpretable models in addition to ensuring model fidelity encapsulated by $\mathcal{L}$. In the case of when G consists of the space of all decision trees, $\Omega(g)$ could be a parameter controlling the maximum depth of the tree g fitted to the black box model f. In the case of logistic regression, it could be a term penalizing the total weight magnitude of g's coefficients to encourage sparse weights. An example of this is the l1 penalty

$$\Omega(g) = \alpha \sum_{w_g} |w_g|, \tag{4}$$

where w_g refer to the weights of the fitted logistic regression model and α controls the weight of regularization.

EXPERIMENTS

We conducted four sets of experiments with the proposed LIME explanations framework on the DHI dataset to demonstrate the utility of interpretability for the application of prospect risking. The first set of experiments aims to explain model decisions for individual examples in the dataset in terms of the features most responsible for the associated model decision. For the purposes of validation, this is first carried out in terms of high-level attributes like initial Pg, DHI Index, final Pg, etc., and secondly in terms of the various low level attributes seismic interpreters have to directly identify and interpret on the acquired geophysical data itself. The basic workflow involves training various machine learning classifiers to predict well outcome

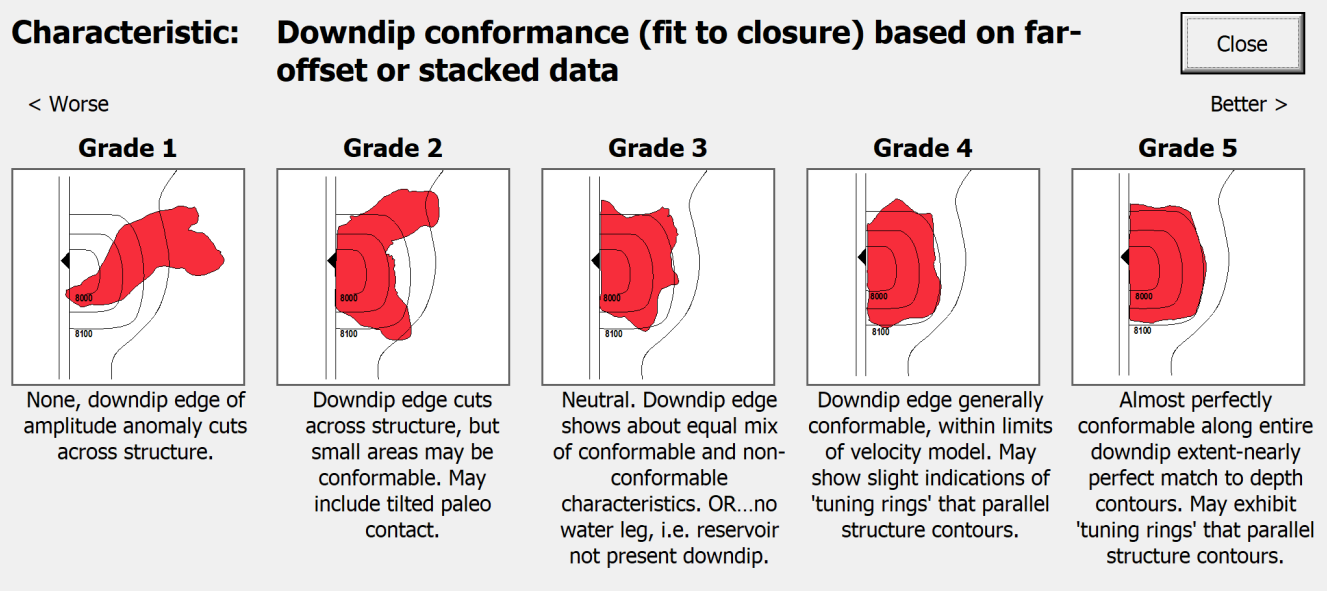

Figure 2: Grading criteria for amplitude downdip conformance from grade 1 to 5. *Source:* Rose & Associates DHI Consortium, 2022, used with permission.

given select features and afterwards using LIME to explain the classifier decision in terms of feature scores (either positive or negative). In the second set of experiments, we perform a case study whereby LIME explanations can help interpreters detect bias in the model arising from spurious correlations in the training dataset. The third set of experiments demonstrates the application of LIME explanations to aid in feature engineering and removal of unnecessary features to reduce the risk of overfitting for a machine learning classifier. Lastly, we show how LIME explanations that are locally faithful to the underlying model on a case-by-case basis can be aggregated to deduce global statistics over the dataset helping in various downstream applications from generating scientific insights to model validation and selection.

Explaining Model Predictions with High level and Low level attributes

From the complete set of input features available in the DHI dataset, we select six features considered to be high-level attributes: initial Pg, DHI index, calibrated Pg, and data quality scores for composite, seismic, and rock and fluid data, respectively (numbered 1 to 6, in this order). A logistic regression classifier is trained to map these features to the outcome class (success or failure) for all AVO class 3 wells. The dataset is split in an 80/20 ratio between training and a hold-out validation set in a random manner. We obtain training and validation set accuracies of 0.82 and 0.81, respectively. Afterwards, LIME explanations are generated for select examples in the validation set. Three such cases are shown in Figure 3. For each instance, LIME fits a linear model in the proximity of the data point of interest as described in the optimization problem in equation 1. The weights assigned to each feature along with the value for the intercept are then displayed in the form of the horizontal bar chart as shown in the figure. Features are ranked in descending order of importance in a top-down fashion as determined by the LIME score. Features assigned a net positive weight (orange bars) correlate positively to the outcome class i.e., a higher value for the feature would tend to bias the classifier more towards the predicted class. Similarly, features assigned a negative weight correlate negatively to the outcome class i.e., a higher value for the feature would tend to swing the classifier away from the predicted class (and vice versa). Numbers inside parentheses next to each feature represent the numerical values associated with the respective feature for the given instance.

Figure 3(a) depicts a ground-truth successful prospect in the validation set that the classifier predicted correctly with high confidence (0.874). A high value for feature 3 (calibrated Pg) is shown to matter the most in terms of deciding the outcome followed by features 1 and 2 (initial Pg and the DHI Index, respectively). A similar trend is observed for the case in Figure 3(b), except that it is *low* values for these features that tend to matter the most to the classifier when deciding if the prospect is a failure. This agrees with intuition since these features are indeed known to correlate very strongly to the outcome as described. LIME explanations thus serve a very useful purpose in verifying a model's reliability by comparing its reasoning process to what is known of prior knowledge. In Figure 3(c), the classifier correctly predicts on a successful prospect but with a low confidence. The reason underpinning this behavior is manifested in the LIME explanation: an unusually high value for feature 5 (seismic data quality) combined with that of initial Pg tends is

compensated for by low values for DHI Index and the final Pg, resulting in an overall weak positive decision. This is an example of where LIME explanations can help make the final decision on an uncertain exploration prospect by looking at the model's explanation. Having validated the utility of LIME on high level features in the DHI dataset, we then repeated the procedure for the low level attributes directly observed and graded by seismic interpreters. To showcase the generalizability of LIME to any classifier of choice, we chose to use a support vector machine to learn the mapping from the low level attributes to the outcome class for all AVO class 3 wells. The SVM obtains training and validation set accuracies of 0.88 and 0.71, respectively. Figure 4 depicts LIME explanations generated for six different instances in the validation set, three for each outcome class. As before, we use a generic identifier with arabic number system to refer to actual features interpreted by geophysicists for ascertaining exploration risk. Each feature is graded on a scale from one to five, unlike high level features before that represented probabilities.

Identifying Bias in the Dataset

Datasets containing spurious correlations among features are a significant risk for machine learning models deployed in the real world. We demonstrate a use case whereby LIME explanations can help users detect any such potential issues. To simulate such a scenario, we introduced an artificial feature into the DHI dataset called 'country ID' that takes one of three possible values: 1, 2, and 3. We then randomly assigned 70% of successful prospects in the dataset to country 1, with all remaining prospects (whether successes or failures) split between countries 2 and 3. We then proceeded to train a classifier on this corrupted dataset as before. Figure 5 depicts two examples from the validation set the classifier of choice predicted correctly on with high confidence: (a) a ground-truth negative and (b) a ground-truth positive. In both cases, it can be observed the country ID (feature 27) plays the most important role among all features in determining the classifier's prediction. Having access to such insights can potentially prevent exploration decisions informed by classifiers trained on biased datasets.

Feature Engineering via LIME Explanations

In large, multidimensional datasets consisting of many features, selecting the right features to use to train a machine learning classifier with can prove to be an arduous task. By ranking features in order of importance for specific data points, LIME explanation lend insight into the underlying physical phenomena and help users choose the most important features for the given application. The DHI dataset collects multiple attributes manually interpreted and graded by seismic interpreters to help decide prospect outcome. At first glance, it is not obvious which ones would be most effective in terms of helping the machine learning model decide the outcome. Figure 4 depicts some of these features as ranked in order of importance for various prospects in the validation set. By observing multiple, select examples, we observed features 3, 4, 5, and 7 to feature very frequently in the corresponding LIME explanations. Accordingly, we pruned the dataset to only these features and retrained in the same fashion as before two classifiers: a support vector machine and a random forest classifier. The training and validation accuracies for each classifier before with all features and afterwards with only the four aforementioned features are listed in Table 1. With SVMs, even though the training set accuracy drops after trimming the number of features, the validation set accuracy stays constant. This reinforces our prior beliefs about the features selected based on LIME scores being important in deciding the outcome for the given prospect over other features. On the other hand, random forests are able to obtain higher training and validation set accuracies with the full set of features (a clear case of overfitting), the drop in performance in both categories is larger when retrained with only four features. Among other things, this helps the interpreter gain an understanding of how the model may be arriving at its reasoning process regardless of the performance scores and therefore in selecting the most optimal model.

	With 31 features		With 4 features	
	Train Acc.	Test Acc.	Train Acc.	Test Acc.
SVMs	0.88	0.71	0.77	0.71
RFs	1.00	0.78	0.82	0.69

Table 1: Feature engineering based off LIME explanations. For both support vector machine and random forest classifiers, we measure the accuracies obtained on training and test sets before and after feature selection using LIME. To what extent they can still maintain their accuracies lends insight into how well they captured the underlying correlations.

Summarizing Global Model Behavior through Aggregation of Local Explanations

Since LIME explanations are generated on individual data points and only capture the behavior of the model's decision boundary in the proximity of those points, there is only so far they can go in terms of providing a full picture of a model's understanding of a dataset. Towards this end, we devised two metrics to help us capture the global model statistics via aggregation of local LIME explanations. The first of these is the *top K relevance score*, a statistic that measures the frequency with which a given feature appears in the top K rankings generated by LIME over the whole dataset. This is computed as

$$\text{top-k}_i = \sum_{x \in \mathcal{D}} \mathbf{1}_{rank(d_i) \leq k}, \tag{5}$$

where d_i refers to the i-th feature in the dataset $D =$

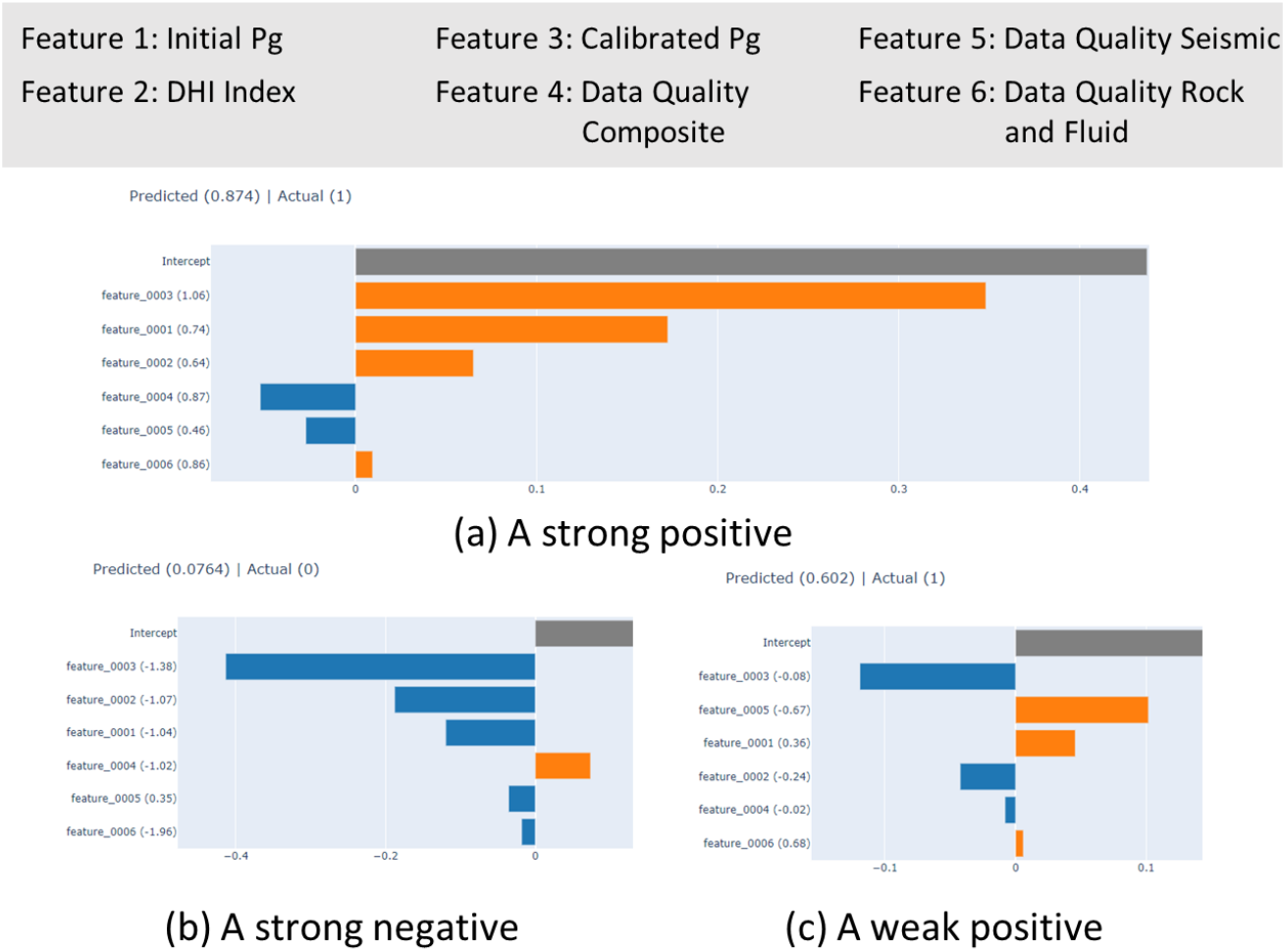

Figure 3: LIME explanations generated for three different examples in the test set for high-level attributes: (a) LR classifier predicts a strong positive for a ground-truth positive prospect (b) LR classifier predicts a strong negative for a ground-truth negative prospect (c) LR classifier predicts a weak positive for a ground-truth positive prospect. Orange bars indicate preference for positive values for features while blue bars indicate a preference for negative values of features for the respective decision.

$\{x\}$. The summation is carried out over all instances where the rank of feature d_i is less than k as determined by LIME. k is a parameter decided by the user. Low values for k result in relevance scores highly able to distinguish between important and unimportant features in the dataset. In column 1 of table 2, this is seen in the relatively high score obtained by feature 3 (calibrated DHI) compared to other features. Higher values for k may be used to obtain features of more secondary importance, especially in cases where there may be no single attribute clearly dominating in terms of single-handedly deciding the outcome. By analyzing the relevace score at different values for k, one can hope to achieve a fuller understanding of the model's behavior over the dataset. In our case, features 3 (calibrated Pg), 2 (DHI index), and 5 (seismic data quality) are seen as important markers of decision outcome based off a global aggregation of LIME explanations. One also has the option to separately analyze for global feature importances for different outcome classes in the dataset, as depicted in table 3. In this case, both outcome classes (well successes and failures) tend to follow the same trends in terms of global feature importance scores.

The second metric we used to establish global importance scores is the *absolute aggregate coefficient (AAC)* obtained as

$$\mathrm{AAC}_{d_i} = \sum_{x \in \mathcal{D}} |w_i^{(x)}|, \tag{6}$$

where d_i as before refers to the i-th feature in the dataset $\mathcal{D} = \{x\}$ and $|w_i^{(x)}|$ refers to the absolute value for the weight assigned by LIME to this feature for example x. The AAC for the six high level features in the dataset is shown for three different classifers (logistic regression, support vector machine, and multilayer perceptron) in table 4. For logistic regression and support vector machine

	Top 1 Relev.	Top 3 Relev.	Top 5 Relev.
Feature 1	1	20	52
Feature 2	3	38	52
Feature 3	48	52	52
Feature 4	0	16	45
Feature 5	0	30	51
Feature 6	0	0	8

Table 2: Top-k relevance statistics for high-level features in the DHI dataset obtained through aggregation of LIME explanations. For a given feature, Top-k relevance score measures the number of times a given feature appeared in the top K feature rankings generated by LIME.

	Successes	Failures
Feature 1	26	19
Feature 2	22	16
Feature 3	30	22
Feature 4	2	2
Feature 5	10	7
Feature 6	0	0

Table 3: Outcome-based analysis with Top-k relevance statistics. For both outcome classes in the dataset (successes and failures), we separately compile global statistics to generate feature importance rankings based on the Top 3 relevance score.

classifiers, it can be seen how they follow similar trends to those observed with the top 3 relevance scores earlier. For MLPs, they are anomalous in that they look at the various features very differently in terms of importance compared to the other two classifers. This is yet again an example of where having a global picture of a model's understanding of a dataset can lead an interpreter to make educated decisions about deploying the most suitable model for the application. Compared to individual explanations, global statistics can provide a quick tool to filter models not aligning to reasoning processes established in prior domain knowledge.

DISCUSSION

The preceding analysis of hydrocarbon risk assessment with LIME explanations sheds light on a variety of ways the proposed tool can be used to aid in exploration tasks. On a basic level, such explanations help the end user better understand the way a complicated black box model might have made the decision on a particular example without access to details of the model's inner workings. This is made possible by fitting interpretable models in the local neighborhood of the query example to mimic the original classifier's decision-making behavior. The output of such explanations is a ranking of features based on the importance scores assigned to them by the fitted interpretable models. This helps firstly to help users validate model decisions before they are acted on by comparing the observed reasoning process to domain-specific prior knowledge. In our case, calibrated Pg (feature 3) was shown to be the most decisive feature when predicting well outcome with high level features, as depicted by Figure 3. This is something well known in risk assessment workflows and helps place trust in the model's decision.

	LR	SVM	MLP
Feature 1	9.05	2.54	1.49
Feature 2	8.86	2.75	0.47
Feature 3	10.53	5.81	1.51
Feature 4	1.31	0.26	2.0
Feature 5	2.63	0.39	1.15
Feature 6	0.53	0.47	1.62

Table 4: Absolute aggregate coefficient statistics for high-level features in the DHI dataset obtained through aggregation of LIME explanations. For a given feature, Absolute aggregate coefficient score measures the sum of absolute values for individual feature scores over the complete dataset.

Beyond this obvious use case however, such explainability-based studies have immense potential to uncover generate new scientific hypotheses regarding the underlying physical phenomena involved. In Figure 4(b), all negative instances are shown to rank features 7, 4, 5, and 3 (in this order) to be among the top five attributes used for arriving at a decision by the model. The frequency with which this pattern appears suggests there might be something going on to explain this phenomenon, potentially opening doors to important scientific discoveries to aid hydrocarbon risk assessment workflows. This is especially important in large multidimensional datasets containing many features where a simple correlation analysis of individual features with the target outcome might not lend much insight.

It was also seen in Figure 5 how LIME helped detect bias in the training dataset and subsequently the model itself. This is in fact a common issue that plagues many machine learning datasets used for day-to-day applications. By uncovering the unusually high statistical correlation between well outcome and the artificially generated country identity feature, LIME helped prevent AI-based decisions that could have been made in the future with such a biased model.

An important consequence of these results is the ability to perform feature engineering and selection for learning a better mapping to the target outcome, as observed in Table 1. By cutting down features based not only on their low importance scores as determined by LIME but also their relevance to the task at hand (e.g., country identity), one can potentially obtain a better training set with lower risk of overfitting.

Lastly, we proposed means whereby the LIME expla-

nations locally faithful to individual instances could be aggregated to compute global statistics over the complete dataset. Where on the one hand this serves to reduce effort by end user spent in analyzing multiple individual explanations, this also provides on the other a unified quantitative approach to better analyze relative importances of features across the dataset and the fidelity of models to underlying scientific prior knowledge. In Table 3, it is made very clear forexample the clear numerical superiority of calibrated Pg over other features in determining the final prospect outcome by the model. Similarly, Table 4 reveals how the particular MLP model might not have learned the underlying causal behaviors governing the dataset dynamics correctly.

CONCLUSION

In this work, we demonstrated the application of the concept of explainable machine learning to hydrocarbon risk assessment systems. In particular, we showed how LIME explanations could be used to generate model-agnostic, local explanations for individual instances in the dataset to uncover insights into the trained model's reasoning process. LIME explanations can provide a unified framework to assess the importance of various features in the dataset as well as to evaluate the fidelity of various trained models to the underlying physical phenomena. This was investigated by means of several studies showing the utility of said method to give insights regarding important features in the dataset, to detect statistical biases in the trained model, and to perform feature selection informed by explainability-based attribute analysis. Finally, we also proposed novel metrics to unify local explanations to give a universal picture of the model's understanding of the target dataset. While this is expected to improve the risk assessment process by helping users place more trust in model predictions, we hope the work will inspire multiple lines of inquiry investigating the utility of explainability to other geoscience applications as well.

REFERENCES

Alaudah, Y., M. Alfarraj, and G. AlRegib, 2019a, Structure label prediction using similarity-based retrieval and weakly supervised label mapping: Geophysics, **84**, no. 1, V67–V79.

Alaudah, Y., P. Michałowicz, M. Alfarraj, and G. AlRegib, 2019b, A machine-learning benchmark for facies classification: Interpretation, **7**, no. 3, SE175–SE187.

Alaudah, Y., M. Soliman, and G. AlRegib, 2019c, Facies classification with weak and strong supervision: A comparative study: SEG Technical Program Expanded Abstracts 2019, Society of Exploration Geophysicists, 1868–1872.

Alfarraj, M., Y. Alaudah, Z. Long, and G. AlRegib, 2018, Multiresolution analysis and learning for computational seismic interpretation: The Leading Edge, **37**, 443–450.

Alfarraj, M., and G. AlRegib, 2019, Semisupervised sequence modeling for elastic impedance inversion: Interpretation, **7**, no. 3, SE237–SE249.

AlRegib, G., and M. Prabhushankar, 2022, Explanatory paradigms in neural networks: arXiv.

Amin, A., M. Deriche, M. A. Shafiq, Z. Wang, and G. AlRegib, 2017, Automated salt-dome detection using an attribute ranking framework with a dictionary-based classifier: Interpretation, **5**, no. 3, SJ61–SJ79.

Bibal, A., M. Lognoul, A. de Streel, and B. Frénay, 2020, Legal requirements on explainability in machine learning: Artificial Intelligence and Law, **29**, 149–169.

Biswas, R., M. K. Sen, V. Das, and T. Mukerji, 2019, Prestack and poststack inversion using a physics-guided convolutional neural network: Interpretation, **7**, no. 3, SE161–SE174.

Di, H., M. Alfarraj, and G. AlRegib, 2018a, Three-dimensional curvature analysis of seismic waveforms and its interpretational implications: Geophysical Prospecting.

Di, H., and G. AlRegib, 2019, Semi-automatic fault/fracture interpretation based on seismic geometry analysis: Geophysical Prospecting, **67**, 1379–1391.

Di, H., M. Shafiq, and G. AlRegib, 2018b, Multi-attribute k-means clustering for salt-boundary delineation from three-dimensional seismic data: Geophysical Journal International, **215**, 1999–2007.

Di, H., M. A. Shafiq, Z. Wang, and G. AlRegib, 2019a, Improving seismic fault detection by super-attribute-based classification: Interpretation, **7**, no. 3, SE251–SE267.

———, 2019b, Improving seismic fault detection by super-attribute-based classification: Interpretation, **7**, no. 3, SE251–SE267.

Du, M., N. Liu, and X. Hu, 2019, Techniques for interpretable machine learning: Communications of the ACM, **63**, 68–77.

Forrest, M., R. Roden, and R. Holeywell, 2010, Risking seismic amplitude anomaly prospects based on database trends: The Leading Edge, **29**, 570–574.

Fuchs, D. J., 2018, The dangers of human-like bias in machine-learning algorithms: Missouri S&T's Peer to Peer, **2**, 1.

Long, Z., Y. Alaudah, M. A. Qureshi, Y. Hu, Z. Wang, M. Alfarraj, G. AlRegib, A. Amin, M. Deriche, S. Al-Dharrab, and H. Di, 2018, A comparative study of texture attributes for characterizing subsurface structures in seismic volumes: Interpretation, **6**, no. 4, T1055–T1066.

McKinney, S. M., M. Sieniek, V. Godbole, J. Godwin, N. Antropova, H. Ashrafian, T. Back, M. Chesus, G. S. Corrado, A. Darzi, M. Etemadi, F. Garcia-Vicente, F. J. Gilbert, M. Halling-Brown, D. Hassabis, S. Jansen, A. Karthikesalingam, C. J. Kelly, D. King, J. R. Ledsam, D. Melnick, H. Mostofi, L. Peng, J. J. Reicher, B. Romera-Paredes, R. Sidebottom, M. Suleyman, D. Tse, K. C. Young, J. D. Fauw, and S. Shetty, 2020, International evaluation of an AI system for breast cancer

screening: Nature, **577**, 89–94.

Mustafa, A., M. Alfarraj, and G. AlRegib, 2019, Estimation of acoustic impedance from seismic data using temporal convolutional network: SEG Technical Program Expanded Abstracts 2019, Society of Exploration Geophysicists, 2554–2558.

Mustafa, A., and G. AlRegib, 2020, Joint learning for seismic inversion: An acoustic impedance estimation case study: SEG Technical Program Expanded Abstracts 2020, Society of Exploration Geophysicists, 1686–1690.

———, 2021, Man-recon: Manifold learning for reconstruction with deep autoencoder for smart seismic interpretation: 2021 IEEE International Conference on Image Processing (ICIP), 2953–2957.

Nosjean, N., R. Holeywell, H. Pettingill, R. Roden, and M. Forrest, 2021, Geological probability of success assessment for amplitude-driven prospects:a nile delta case study: Journal of Petroleum Science and Engineering, **202**, 108515.

Prabhushankar, M., G. Kwon, D. Temel, and G. AlRegib, 2020, Contrastive explanations in neural networks: 2020 IEEE International Conference on Image Processing (ICIP), IEEE, 3289–3293.

Roden, R., M. Forrest, and R. Holeywell, 2012, Relating seismic interpretation to reserve/resource calculations: Insights from a dhi consortium: The Leading Edge, **31**, 1066–1074.

Roden, R., M. Forrest, R. Holeywell, M. Carr, and P. A. Alexander, 2014, The role of avo in prospect risk assessment: Interpretation, **2**, SC61–SC76.

Roscher, R., B. Bohn, M. F. Duarte, and J. Garcke, 2020, Explainable machine learning for scientific insights and discoveries: IEEE Access, **8**, 42200–42216.

Rose, P. R., 1992, *in* Chance of Success and Its Use in Petroleum Exploration: Chapter 7: Part II. Nature of the Business.

Selvaraju, R. R., M. Cogswell, A. Das, R. Vedantam, D. Parikh, and D. Batra, 2017, Grad-cam: Visual explanations from deep networks via gradient-based localization: Proceedings of the IEEE international conference on computer vision, 618–626.

Shafiq, M. A., Z. Wang, G. AlRegib, A. Amin, and M. Deriche, 2017, A texture-based interpretation workflow with application to delineating salt domes: Interpretation, **5**, no. 3, SJ1–SJ19.

Tjoa, E., and C. Guan, 2021, A survey on explainable artificial intelligence (xai): Toward medical xai: IEEE Transactions on Neural Networks and Learning Systems, **32**, 4793–4813.

Wang, Z., T. Hegazy, Z. Long, and G. AlRegib, 2015, Noise-robust detection and tracking of salt domes in postmigrated volumes using texture, tensors, and subspace learning: Geophysics, **80**, WD101–WD116.

Zhang, Y., K. Song, Y. Sun, S. Tan, and M. Udell, 2019, " why should you trust my explanation?" understanding uncertainty in lime explanations: arXiv preprint arXiv:1904.12991.

REFERENCES FOR GENERAL READING

Aribido, O.J., G. AlRegib, and Y. Alaudah, 2021, Self-Supervised Delineation of Geological Structures using Orthogonal Latent Space Projection: Geophysics, vol. 86, no. 6, V497-V508.

Aribido, O.J., G. AlRegib, and M. Deriche, 2020, Self-Supervised Annotation of Seismic Images Using Latent Space Factorization: IEEE International Conference on Image Processing (ICIP).

Benkert, R., O.J. Aribido, and G. AlRegib, 2021, Example Forgetting: A Novel Approach to Explain and Interpret Deep Neural Networks in Seismic Interpretation: IEEE Transactions on Geoscience and Remote Sensing (TGRS) (submitted).

Benkert, R., M. Prabhushankar, and G. AlRegib, 2022, Reliable Uncertainty Estimation for Seismic Interpretation with Prediction Switches: SEG Technical Program Expanded Abstracts 2020, Society of Exploration Geophysicists.

Benkert, R., O.J. Aribido, and G. AlRegib, 2021, Explaining Deep Models Through Forgettable Learning Dynamics: IEEE International Conference on Image Processing (ICIP).

Di, H., D. Gao, and G. AlRegib, 2019, Developing a Seismic Texture Analysis Network for Automated Seismic Pattern Recognition and Classification: Geophysical Journal International, vol. 218, no. 2, pp. 1262-1275.

Di, H., and G. AlRegib, 2019, Semiautomatic Fault/Fracture Interpretation Based on Seismic Geometry Analysis: Geophysical Prospecting, vol. 67, no. 5, pp. 1379-1391.

Di, H., and G. AlRegib, 2019, Reflector Dip Estimates Based on Seismic Waveform Curvature/Flexure Analysis: Interpretation, vol. 7, no. 2, pp. SC1-SC9.

Hu, Y., Z. Wang, and G. AlRegib, 2020, Texture Classification Using Block Intensity and Gradient Difference (BIGD) Descriptor: Signal Processing: Image Communication.

Hu, Y., Z. Long, A. Sundaresan, M. Alfarraj, G. AlRegib, S. Park, and S. Jayaraman, 2020, Fabric Surface Characterization: Assessment of Deep Learning-Based Texture Representations Using a Challenging Dataset: The Textile Institute.

Kwon, G., M. Prabhushankar, D. Temel, and G. AlRegib, 2020, Backpropagated Gradient Representations for Anomaly Detection: Proceedings of the European Conference on Computer Vision (ECCV).

Kwon, G., M. Prabhushankar, D. Temel, and G. AlRegib, 2020, Novelty Detection Through Model-Based Characterization of Neural Networks: IEEE International Conference on Image Processing (ICIP).

Kwon, G., and G. AlRegib, 2022, A Gating Model for Bias Calibration in Generalized Zero-Shot Learning: IEEE Transactions on Image Processing (TIP).

Kokilepersaud, K., M. Prabhushankar, and G. AlRegib, 2022, Volumetric Supervised Contrastive Learning for Seismic Semantic Segmentation: SEG Technical Program Expanded Abstracts 2020, Society of Exploration Geophysi-

cists.
Lee, J., C. Lehman, and G. AlRegib, 2021, Towards Understanding the Purview of Neural Networks via Gradient Analysis: IEEE Transactions on Neural Networks and Learning Systems (TNNLS).
Mustafa, A., M. Alfarraj, and G. AlRegib, 2020, Spatiotemporal Modeling of Seismic Images for Acoustic Impedance Estimation: SEG Technical Program Expanded Abstracts 2020, Society of Exploration Geophysicists.
Mustafa, A., and G. AlRegib, 2022, Active Learning With Deep Autoencoders for Seismic Facies Interpretation: Geophysics (submitted).
Lee, J., and G. AlRegib, 2020, Gradients as a Measure of Uncertainty in Neural Networks: IEEE International Conference on Image Processing (ICIP).
Lehman, C., D. Temel, and G. AIRegib, 2020, "On the Structures of Representation for the Robustness of Semantic Segmentation to Input Corruption," in IEEE International Conference on Image Processing (ICIP).
Liu, S., C. Lehman, and G. AlRegib, 2020, Robustness and Overfitting Behavior of Implicit Background Models: IEEE International Conference on Image Processing (ICIP).
Mustafa, A., and G. AlRegib, 2022, Advances in Deep Learning-Based Seismic Inversion: A Review, Geophysics (submitted).
Prabhushankar, M., and G. AlRegib, 2022, Stochastic Surprisal: An Inferential Measurement of Free Energy in Neural Networks: Frontiers in Neuroscience – Perception Science (submitted).
Prabhushankar, M., G. Kwon, D. Temel, and G. AlRegib, 2020, Contrastive Explanations in Neural Networks: IEEE International Conference on Image Processing (ICIP).
Shafiq, M., Z. Long, H. Di, and G. AlRegib, 2021, A Novel Attention Model for Salient Structure Detection in Seismic Volumes: Applied Computing and Intelligence.
Soliman, M., C. Lehman, and G. AlRegib, 2020, S6: Semi-Supervised Self-Supervised Semantic Segmentation: IEEE International Conference on Image Processing (ICIP).
Sun, Y., M. Prabhushankar, and G. AlRegib, 2019, Implicit Saliency in Deep Neural Networks: IEEE International Conference on Image Processing (ICIP).
Temel, D., M. J. Mathew, G. AlRegib, and Y. M. Khalifa, 2019, Relative Afferent Pupillary Defect Screening Through Transfer Learning: IEEE Journal of Biomedical and Health Informatics.
Temel, D., M-H. Chen, and G. AlRegib, 2019, Traffic Sign Detection Under Challenging Conditions: A Deeper Look Into Performance Variations and Spectral Characteristics: IEEE Transactions on Intelligent Transportation Systems.

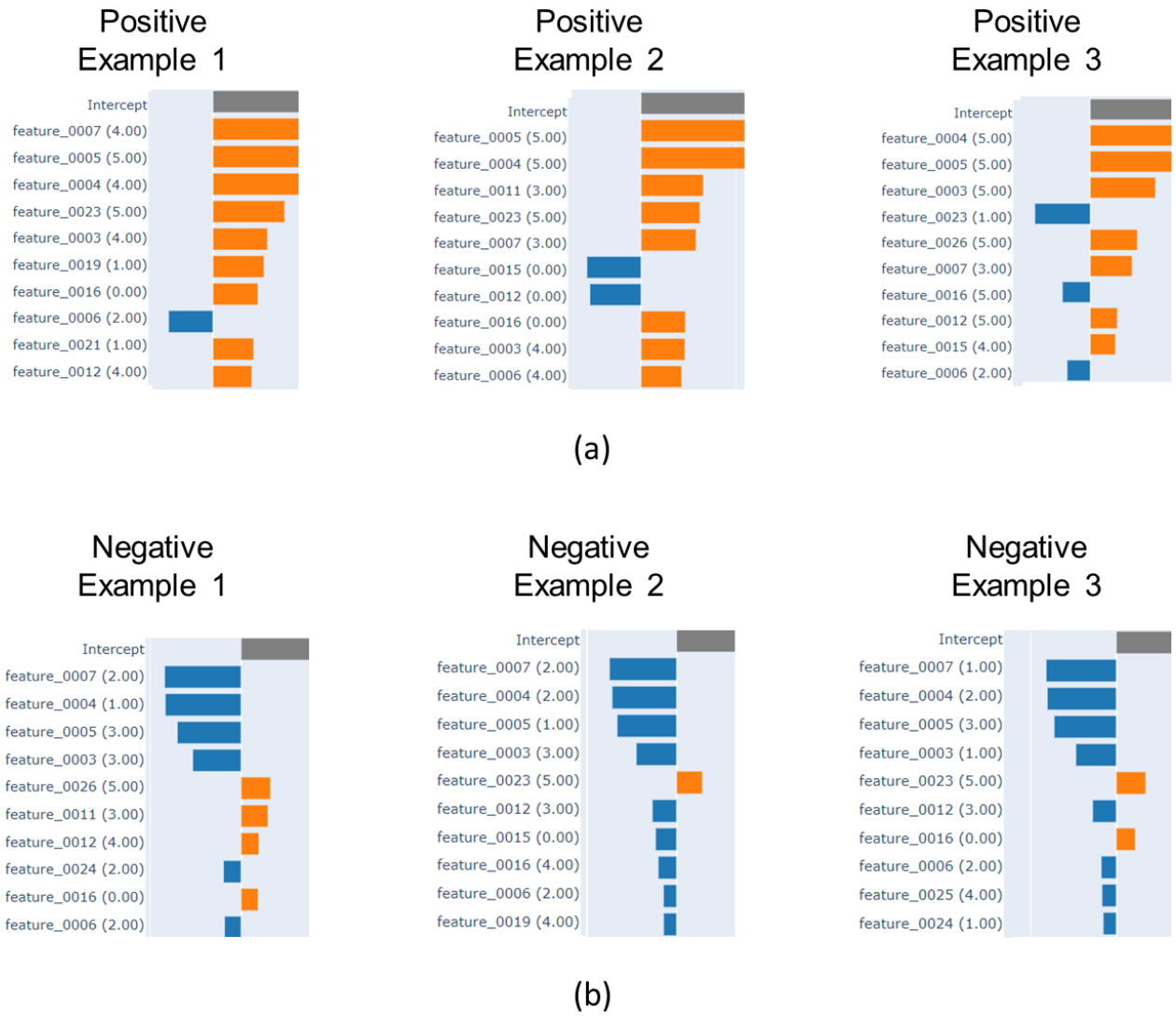

Figure 4: LIME explanations generated six instances in two ground-truth classes in the test set for low-level attributes: (a) SVM predicted positive for ground-truth positive class (b) SVM predicted negative for ground-truth negative class. Orange bars indicate preference for positive values for features while blue bars indicate a preference for negative values of features for the respective decision. For the sake of brevity, only the top 10 features are shown for each explanation.

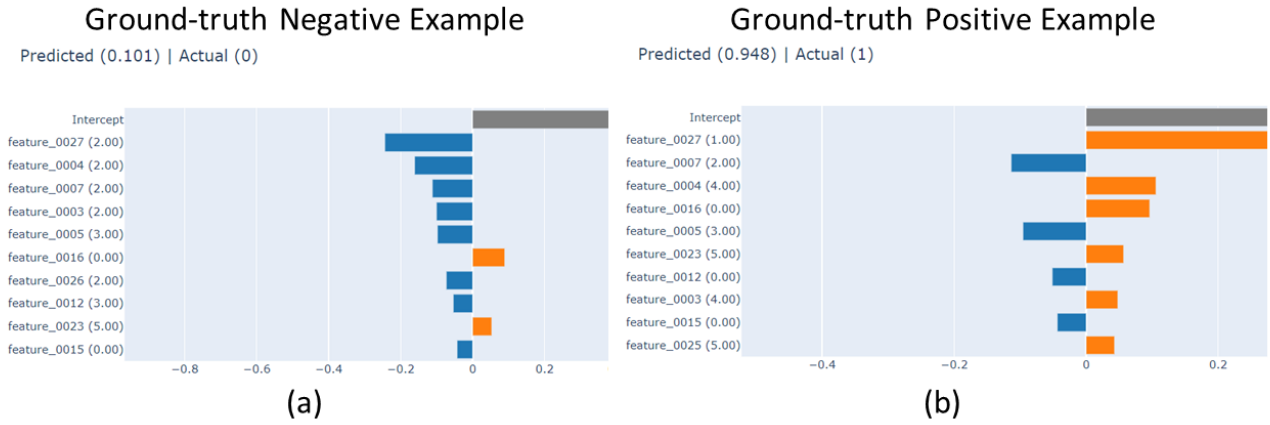

Figure 5: LIME explanations generated for a machine learning classifier trained on the 'corrupted' DHI dataset with low level attributes. (a) A ground-truth positive predicted as positive by the classifier. (b) A ground-truth negative predicted as negative by the classifier. LIME explanations reveal the classifier's over-reliance on the 'country ID' (feature 27) to make outcome decisions for the prospect.